www.vbripress.com/aml, DOI: 10.5185/amlett.2016.6850 Published online by the VBRI Press in 2016

Eco-friendly approach: Graphene like boron nitride modified calcium material for the synthesis of 2-amino-4H-pyran-3-carbonitrile derivatives

T. Muthu, K. Anand, M. Sureshkumar, R. M. Gengan*

Department of Chemistry, Faculty of Applied Sciences, Durban University of Technology, Durban 4001, South Africa

*Corresponding author. Tel: (+27) 31 3732309; Fax: (+27) 31 2022671; E-mail: genganrm@dut.ac.za

Received: 09 April 2016, Revised: 06 June 2016 and Accepted: 17 June 2016

ABSTRACT

An efficient one-pot multi-component synthesis of medicinally important 2-amino-4H-pyran-3-carbonitrile derivatives using a new heterogeneous calcium loaded boron nitride (CaBNT) catalyst is described herein. This transformation transpires by Knoevenagel condensation, Michael addition and intramolecular cyclization. Alkaline earth metal-based green catalyst was successfully prepared and characterized by XRD, SEM with EDX, Raman spectroscopy, BET, DSC-TGA and FT-IR. The reaction works up is facile and CaBNT catalyst can easily be separated from the reaction mixture and re-used more than five times in subsequent reactions. This methodology offers several advantages such as excellent yields, use of inexpensive solvent and relatively shorter reaction time. Copyright © 2016 VBRI Press.

Keywords: Heterogeneous catalyst; calcium; boron nitride; multi-component synthesis.

Introduction

One-pot multi-component reactions (MCRs) are simple and efficient synthetic routes for sustaining diverse heterocycles. These reactions are a straight forward one-step transformation which offers significant advantages over conventional linear type synthesis due to its flexible, convergent and atom efficient nature. Thus, the development of multi-component reactions has attracted considerable attention from the view of ideal synthesis by virtue of their efficiency, facile implementation and generally high yield of the products. These reactions are designed to produce elaborate biologically active compounds hence are an important area of research in organic, combinatorial and medicinal chemistry.

The known multi-component procedures for the synthesis of 2-amino-4H-pyran-3-carbonitriles employ a three-component condensation of cyclic 1,3-diketones, aldehydes and malononitrile and is performed under a variety of reaction conditions. Catalysts such as piperidine/ammonium acetate [**1**], triethylamine [**2**] are reported and the yields are in the range of 70-85 %. Alkyl ammonium salts in water [**3**], (S)-proline in aqueous media [**4**] afford the corresponding carbonitriles in higher yields (75-95 %), however they suffer from long reaction times up to 10 hours. As a consequence, reagents such as benzyltriethylammonium chloride (TEBA) [**5**], NaBr [**6**], microwave irradiation [**7**] and amino functioned ionic liquid [**8**] are reported to catalyze these reactions including ammonium chloride [**9**], ethylenediamine diacetate [**10**], surfactant metal carboxylates [**11**] and b-cyclodextrin [**12**]. However, some of the reporting procedures have drawbacks such as tedious work-up, use of expensive reagents, long reaction times and low yields of products.

Insulating oxides such as SiO_2, Al_2O_3, silica-alumina and various zeolites are the materials commonly used as catalyst supports [**13**]. These oxides possess low thermal conductivity, generating sintering of the assisted metal on hot spots, various acidic and basic sites and the coverage of the catalyst with water at low temperature due to its hydrophilic surface. Various two-dimensional (2D) nanomaterials have received considerable developments for heterogeneous catalysis. Among them, boron nitride has attracted more attention because of its high elastic modulus, high melting-point, excellent thermal conductivity and a large and direct band gap. Such properties can be of high value for ultraviolet-light emitters, advanced ceramic composites, electrical insulators, solid lubricants and ideal substrates [**14**] so we have fixed boron nitride (BNT) as catalyst support. The graphene like hexagonal boron nitride [**15**] is a most stable isomer. A giant planar network of hexagonal boron nitride has an acid-base resistance, good thermal and electrical conductivity and chemically very inert. Moreover, BNT is hydrophobic, hence preventing moisture condensation on its surface. Activated BNT exhibits an excellent adsorption performance for various metal ions such as Cr^{3+}, Co^{2+}, Ni^{2+}, Ce^{3+}, Pb^{2+} and organic pollutants (tetracycline, methyl orange and congo red) in water, as well as volatile organic compounds (benzene) in air [**16**].

Herein we report the synthesis and characterization of a new calcium loaded boron nitride catalyst which is subsequently used for a one-pot three component synthesis of 2-amino-4H-pyran-3-carbonitrile derivatives.

Experimental

Materials and methods

All chemicals were purchased from Sigma-Aldrich and used without further purification. Solvents used were of analytical grade. Melting points were determined by Stuart SMP10 and are uncorrected. IR spectra were recorded on KBr discs on a Varian Scimitar 1000 FT-IR and Perkin Elmer. The values are expressed as ν_{max} cm^{-1}. ^{1}H-NMR and ^{13}C-NMR spectra were recorded on BRUKER 400 MHz spectrometer using tetramethylsilane (TMS) as an internal standard. The chemical shift values are recorded on δ scale and the coupling constants (J) are in hertz. The DSC-TGA analysis was conducted with TA Instruments. The X-ray diffraction analysis was conducted with a Philips PW 1050 diffractometer set at 1min with a scanning step size of 0.02º from 40º to 100º 2Θ using monochromated Cok_{α} radiation. Data were captured with a sietonics 122D automated microprocessor linked to the diffractometer. A Carl Zeiss Ultra Plus scanning electron microscope with EDX detector was used. The progress of the reaction was monitored by TLC using aluminium plates with silica gel (Sigma Aldrich).

Preparation of calcium loaded boron nitride catalyst

To a solution of $Ca(OAc)_2$ (19.7 mg, including 7.6 % mg of Ca metal; 0.5 wt % of Ca metal vs. BNT) in methanol (50 mL) was added boron nitride (2.66 g) and the deferment was stirred at room temperature for a week. The resulting suspension was filtered and the solid was washed with MeOH, dried under reduced pressure to yield 0.3 % CaBNT catalyst as a white powder; yield: 2.679 g.

General procedure for the preparation of 2-amino-4(H)-pyran-3-carbonitrile derivatives

In a 100 mL round bottom flask, a mixture of an aryl aldehyde (1 mmol), malononitile (1 mmol) and CaBNT (0.10 g, 10 mol % of the substrate) in ethanol (15 mL) was refluxed with stirring on an oil bath. After one hour, 5, 5-dimethylcyclohexane-1, 3-dione was added. The progress of the reaction was monitored by TLC. After completion of the reaction, the solvent was allowed to evaporate. The product was purified by column chromatography (eluent ethyl acetate: petroleum ether, 50 %). The catalyst was recovered by filtration. The products were characterized by IR, ^{1}H-NMR and ^{13}C-NMR.

Results and discussion

The study was initiated by the synthesis of a new heterogeneous catalyst containing calcium and boron nitride which was prepared by stirring at inert atmosphere for 7 days. The CaBNT was characterized by several techniques: XRD analysis, SEM with EDX, BET analysis, Raman spectroscopy, DSC-TGA and FTIR. XRD analysis of the catalyst (**Fig. 1**) showed the crystalline nature of CaBNT; the characteristic Bragg's XRD peaks at 26.09, 41.05, 54.43 and 75.34 respectively and are indexed to (0 0 2), (1 0 0), (0 0 4) and (2 2 0) whilst Ca peaks at 43.19 and 49.56 were indexed to (1 1 0), (1 1 2).

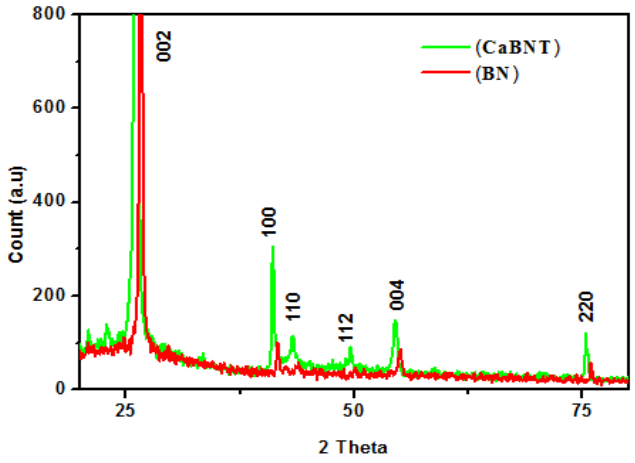

Fig. 1. XRD characterization for calcium loaded boron nitride catalyst.

Fig. 2(A, B) illustrated the SEM morphologies of CaBNT at 1 µm and 2 µm range. The plates like structures are clearly visible. The spherical shaped particles can be observed in the image could be explained as molten B_2O_3 particles that were not converted into BNT during synthesis. **Fig. 2C** showed the Energy Dispersive X-ray (EDX) spectrum of the catalyst. The Ca peaks were observed at 0.3, 3.7 and 4.0 KeV respectively. The appearance of Au peaks is due to the coating with gold during sample preparation.

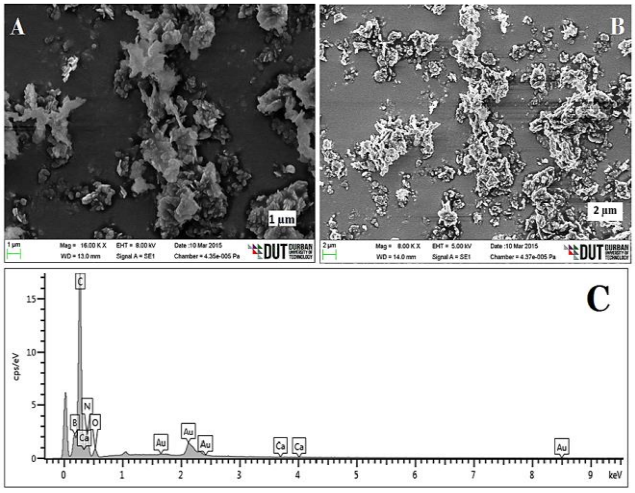

Fig. 2. SEM image for calcium loaded boron nitride at 1 µm (**A**) and 2 µm (**B**) and EDX spectrum (**C**).

Brunauer-Emmett-Teller (BET) analysis showed the specific surface area of CaBNT by nitrogen multilayer adsorption. **Fig. 3** illustrated the nitrogen adsorption and desorption isotherm and the pore size distribution for the catalyst. The observed BET surface area for CaBNT was 21.52m^2/g, pore volume 0.1028cm^3/g and pore size 191.15 A°.

Raman Spectrum of the CaBNT (**Fig. 4**) clearly showed three peaks located at approximately 900 cm^{-1}, 1380 cm^{-1} and 1795 cm^{-1} for BNT with Ca metal. The peak at 1380 cm^{-1} is identified with BNT phonon mode [**17**] whilst the peaks observed at 900 cm^{-1} and 1795 cm^{-1} are related to the component of boron, nitrogen and calcium.

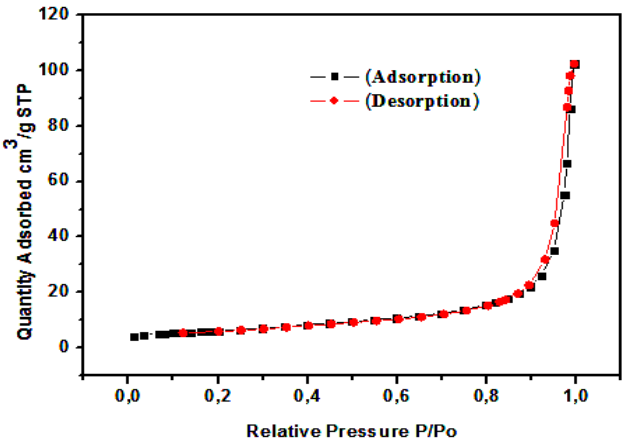

Fig. 3. BET surface area and surface size for calcium loaded boron nitride.

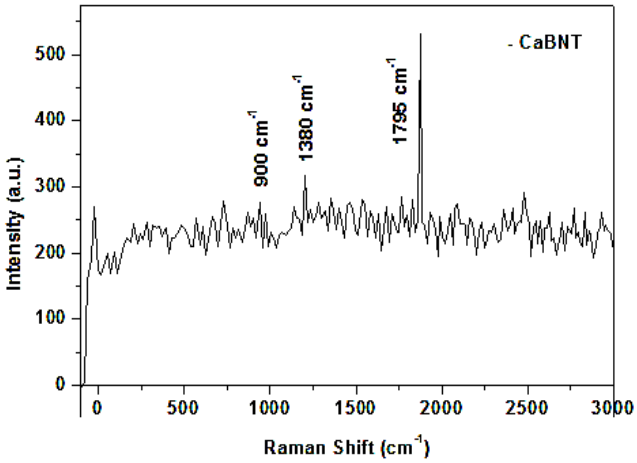

Fig. 4. Raman spectrum for calcium loaded boron nitride.

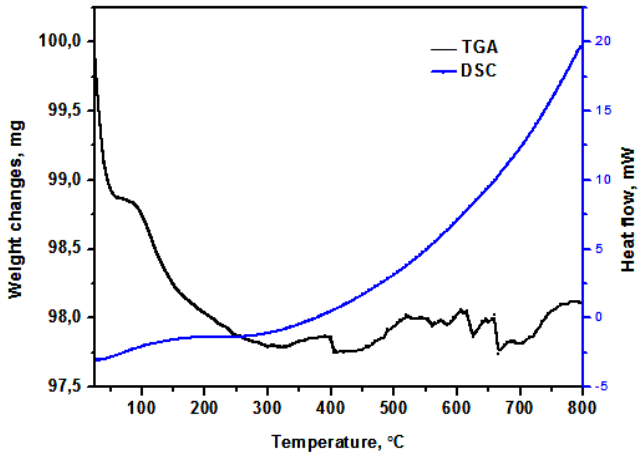

Fig. 5. DSC-TGA for calcium loaded boron nitride catalyst.

The thermal stability of the synthesized CaBNT catalyst was measured from room temperature to 800 ˚C (**Fig. 5**). A broad exothermic peak on the DSC curve was observed at 150 ˚C. The corresponding TGA curve revealed two mass loss viz., 19.34 wt % in the temperature range of 93 to 95 ˚C and 29.98 wt % in the temperature 102 to 300 ˚C which was due to the partial decomposition of the CaBNT. A mass loss of water was observed at 100 ˚C. Above 400 ˚C the weight was found to slightly increase (~ 1.5 wt.%) which may be associated with the partial formation of Ca_3N_2.

Table 1. Effect of optimization of CaBNT catalyst.

Entry	Catalyst	Mol %	Time (h)	Yield (%)
1	BNT	25	upto 24	Trace
2	CaBNT	5	6	70
3	CaBNT	10	6	95
4	CaBNT	15	6	95
5	CaBNT	20	6	95

Fig. 6. Illustrated the Fourier transform infrared (FTIR) spectrum of the CaBNT. The pure BNT possesses richer surface bonds, such as N-B-N (1630 cm^{-1}), B-N (1530 cm^{-1}), B-N-B (814 cm^{-1}) whilst Ca-N (940 cm^{-1}, ant symmetric and 1532 cm^{-1}, symmetric) stretching frequencies exhibit an increase with increased electron-donating capacity as reflected by the Hammett substituent constant [**18**].

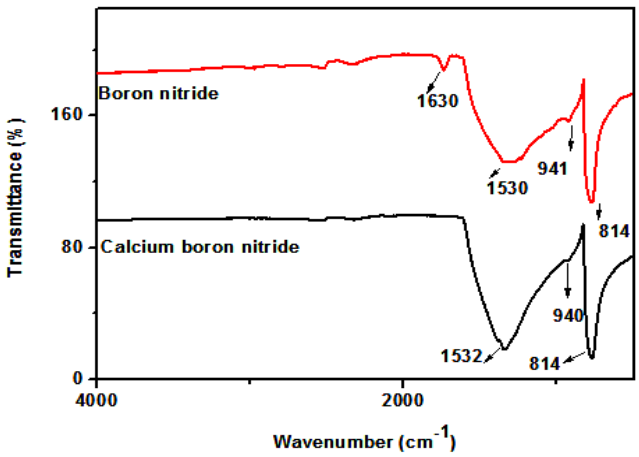

Fig. 6. FT-IR spectrum for calcium loaded boron nitride catalyst.

Thereafter we used the novel catalyst for the synthesis 2-amino-4H-pyran-3-carbonitrile derivatives by means of one-pot, three component condensation of aromatic aldehydes, malononitile and dimedone in ethanol medium (Scheme 1).

In an initial experiment, an equivalent mixture of benzaldehyde 1a (1 mmol), malononitile 2a and dimedone 3a in presence of boron nitride in toluene at 110 °C proceed to completion in 24 hours to afford trace amounts of 4a (R_1=H). When the same substrate mixture was reacted in presence of CaBNT catalyst (5 mol %), the yield of the product 4a was 70 %. In another attempt, in the presence of (10 mol %) catalyst, the yield of the product 4a substantially increased to 95 % within 6 hrs (**Table 1**, entry 3). However, on further increasing the amount of the catalyst to 15 mol% and 20 mol % respectively, no improvement in the yield was observed (**Table 1**, entries 4 and 5). This shows that the best yield of the product was obtained when the catalyst is taken at 10 mol %. This

protocol was used with the appropriate starting compounds to synthesize 4j-n. The structures of the products (**4a-n**) were deduced from their IR, ^{1}H-NMR, ^{13}C-NMR and physical data (mp.) with those reported in the literatures **(Supplementary data)**.

Table 2. Effect of different solvent system on reaction.

Entry	Solvent	Time (h)	Yield (%)
1	DCM	10	80
2	Ethyl Acetate	8	85
3	Ethanol	6	95
4	Acetonitrile	6	80
5	Toluene	8	78
6	Methanol	10	75
7	Water	10	72

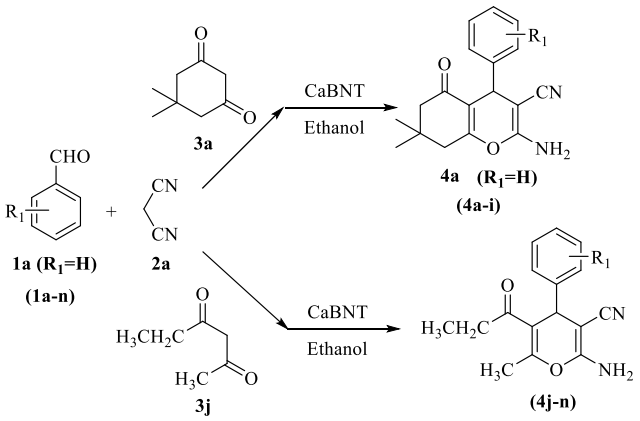

Scheme 1. Three component synthesis of 2-amino-4H-pyran-3-carbonitriles.

Also the model reaction in presence of 10 mol % of the catalyst was carried out at different solvents to assess the effect on the reaction yield. We investigated different solvents such as dichloromethane, ethyl acetate, ethanol, acetonitrile, toluene, methanol and water (**Table 2**). Ethanol was found to be the ideal solvent for this domino reaction which afforded maximum yield of 4a (**Table 2**, entry 3) for 6 hours under reflux at 110 °C. Increasing the reaction time or temperature did not improve the yield. Subsequently, all the syntheses mentioned above were carried out at 110 °C with 10 mol % of CaBNT. The separated catalyst was washed with MeOH followed by drying in an oven at 100°C.

The reusability of the catalyst is one of the most important benefits and makes them useful for commercial applications. To investigate the catalytic efficiency of recycled catalyst, five successive cycles of the model reaction of benzaldehyde, malononitile and dimedone in ethanol (**Scheme 1**) were run under the optimal reaction conditions using recycled CaBNT. The activity of the catalyst did not show any significant decrease in the yields after five successive runs for the model reaction. It was observed that the catalyst displayed good reusability (**Fig.7**).

In order to show the accessibility of the present work, we compared the results with the previously reported catalysts for the preparation of 2-amino-4(H) pyran-3-carbonitrile derivatives.

It should be noted that the reaction time is longer and the percentage yield is less for some catalysts mentioned in **Table 3**.

Table 3. Effect of comparison of reported catalysts with CaBNT heterogeneous catalyst.

Entry	Catalyst	Condition	Solvent	Time	Yield (%)	Refs
1	NaOH/Piperidine	MW	EtOH	5-9 h	71	19
2	KF-Al_2O_3	Reflux	DMF	10-14 h	90	20
3	HTMAB	Reflux	Water	8 h	93	21
4	L-proline	Reflux	EtOH	4 h	90	22
5	$RE(PFO)_3$	Reflux	EtOH	5 h	90	23
6	Trifluoroethanol	Reflux	EtOH	5 h	90	24
7	I_2	Reflux	DMSO	4 h	86	25
8	CaBNT	Reflux	EtOH	6 h	95	This work

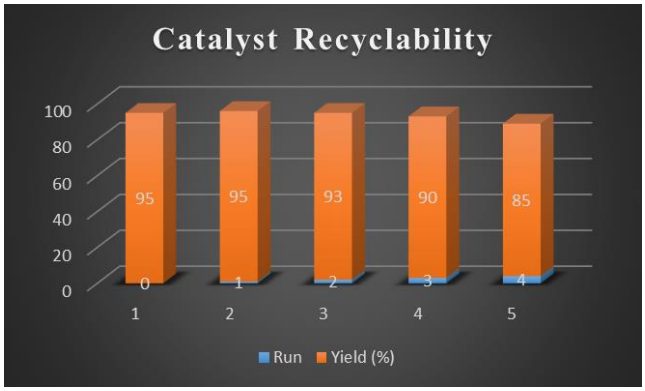

Fig. 7. Recyclability of the calcium loaded boron nitride catalyst.

Also, catalysts such as L-proline, $RE(PFO)_3$, trifluoroethanol and iodine was offered 90 % of yield in less reaction times. The adopted procedure provided a way to compare the effectiveness of CaBNT with other reported catalysts and 95 % of yield was observed in relatively shorter reaction time.

Table 4. Synthesis of compounds (4a-n) from aldehydes, malononitrile and 1,3-dicarbonyl compounds (dimedone and ethyl acetoacetate) under reflux conditions in presence of 10 mol % CaBNT.

Entry	Ar	1,3-diketone	Product	Yield (%)	Melting Point (℃) Observed	Reported
1	H (1a)	$C_8H_{12}O_2$	**4a**	95	233-235	234-235 [26]
2	4-NO_2 (1b)	$C_8H_{12}O_2$	**4b**	95	176-178	177-178 [27]
3	4-FB (1c)	$C_8H_{12}O_2$	**4c**	85	199-201	200 [28]
4	4-MeO (1d)	$C_8H_{12}O_2$	**4d**	80	199-201	199-200 [28]
5	2-NO_2 (1e)	$C_8H_{12}O_2$	**4e**	94	223-226	224-226 [29]
6	4-ClB (1f)	$C_8H_{12}O_2$	**4f**	94	208-210	209-210 [30]
7	4-Me (1g)	$C_8H_{12}O_2$	**4g**	90	219-222	220-222 [31]
8	2-OH (1h)	$C_8H_{12}O_2$	**4h**	75	175-177	–
9	Furfural (1i)	$C_8H_{12}O_2$	**4i**	94	215-217	216 [32]
10	H (1j)	$C_6H_{10}O_3$	**4j**	95	194-196	– [33]
11	4-NO_2 (1k)	$C_6H_{10}O_3$	**4k**	94	177-179	–
12	4-FB (1l)	$C_6H_{10}O_3$	**4l**	83	159-161	– [33]
13	2-NO_2 (1m)	$C_6H_{10}O_3$	**4m**	94	176-178	–
14	4-Me (1n)	$C_6H_{10}O_3$	**4n**	75	171-173	–

Conclusion

In conclusion, we have developed a facile and convenient practical method for easy access to a wide range of pharmaceutically interesting functionalized 2-amino-4H-pyran-3-carbonitriles in the presence of CaBNT via. A one-

pot tandem Knoevenagel-cyclocondensation of aldehydes, malononitile and 1, 3-diketone in ethanol at room temperature. Mild reaction conditions, excellent yields, operational simplicity, clean reaction profiles as well as the use of inexpensive solvent and catalysts are the key advantages of the present method. Moreover, reusability of the catalyst is an added advantage to this protocol. Keeping in mind that the synthetic importance of such biologically relevant pyran-annulated heterocyclic scaffolds directly relate to medicinal chemistry, the present methodology with mild reaction conditions and operational simplicity offers the possibility of its use with cost-effective way for large-scale industrial syntheses as well.

Acknowledgements

We are grateful to the National Research Foundation (NRF) and Durban University of Technology (DUT) for funding this project.

References

1. Hassanien, A.A.; Zahran, M.A.; El-Gaby, M.S.A.; Ghorab, M.M; *J. Indian Chem. Soc.*, **1999**, *76*, 350. **DOI:** 10.1002/chin.200042139
2. Shestopalov, A.M.; Emelianova, Yu.M.; Nesterov, V.N; *Russ. Chem. Bull.*, **2003**, *52*, 1164. **DOI:** 10.1023/A:1024721710597
3. Balalaie, S.; Bararjanian, M.; Amani, A.M.; Movassagh, B; *Syn.lett.*, **2006**, *107*, 263. **DOI:** 10.1055/s-2006-926227
4. Fan, X.; Hu, X.; Zhang, X.; Wang, J; *Aust. J. Chem.*, **2004**, *57*, 1067. **DOI:** 10.1071/CH04060
5. Ablajan, K.; Liju, W.; Tuoheti, A.; Kelimu, Y; *Let. Org. Chem.*, **2012**, *9*, 639. **DOI:** 10.2174/157017812803521135
6. Devi, I.; Bhuyan, P.J; *Tet. Lett*. **2004**, *45*, 8625. **DOI:** 10.1016/j.tetlet.2004.09.158
7. Tu, S.J.; Gao, Y.; Guo, C.; Shi, D.; Lu, Z; *Syn. Comm*., **2002**, *32*, 2137. **DOI:** 10.1081/SCC-120005420
8. Penjg, Y.; Song, G; *Catal. Comm*., **2007**, *8*, 111. **DOI:** 10.1016/j.catcom.2006.05.031
9. Dabiri, M.; Bahramnnejad, M.; Baghbanzadeh, M; *Tetrahedron*., **2009**, *65*, 9443. **DOI:** 10.1016/j.tet.2009.08.070
10. Lee, Y.R.; Hari, G.S; *Synthesis*. **2010**, *3*, 453. **DOI:** 10.1055/s-0029-1217116
11. Wang, L.M.; Jiao, N.; Qiu, J.; Yu, J.J.; Liu, J.Q.; Guo, F.L.; Liu, Y; *Tetrahedron*., **2010**, *66*, 339. **DOI:** 10.1016/j.tet.2009.10.091
12. Sridhar, R.; Srinivas, B.; Madhav, B.; Reddy, V.P.; Nageswar, Y.V.D.; Rao, K; *Can, J. Chem*., **2009**, *87*, 1704. **DOI:** 10.1139/v09-137
13. Spivey, J.J; *Ind. Eng. Chem. Res*., **1987**, *26*, 2165. **DOI:** 10.1021/ie00071a001
14. Liu, F.; Mo, X.; Gan, H.; Guo, T.; Wang, X.; Chen, B; Chen, J.; Deng, S.; Xu, N.; Sekiguchi, T.; Golberg, D.; Bando, Y; *Sci. Rep*., **2014**, *4*, 4211. **DOI:** 10.1038/srep04211
15. Nag, A.; Raidongia, K.; Hembram, K.P.S.S.; Datta, R.; Waghmare, U.V.; Rao, C.N.R; *ACS Nano*., **2010**, *4*, 1539. **DOI:** 10.1021/nn9018762
16. Li, J.; Xiao, X.; Xu, X.; Lin, J.; Huang, Y.; Xue, Y.; Jin, P.; Zou, J.; Tang, C; *Sci. Rep*. **2013**, *3*, 3208. **DOI:** 10.1038/srep03208
17. Kalay, S.; Yilmaz, Z.; Culha, M; *Beilstein J. Nanotechnol*. **2013**, *4*, 843. **DOI:** 10.3762/bjnano.4.95
18. Zhi, C.Y.; Bando, Y.; Tang, C.C.; Golberg, D; *Appl. Phys. Lett*., **2005**, *86*, 213110. **DOI:** 10.1063/1.1938002
19. Zhou, J.F; *Syn. Comm*. **2003**, *33*, 99. **DOI:** 10.1081/SCC-120015564
20. Wang, X.S.; Shi, D.Q.; Du, Y.; Zhou, Y.; Tu, S.J; *Syn. Comm*. **2004**, *34*, 425. **DOI:** 10.1081/SCC-120030692
21. Jin, T.S.; Liu, L.B.; Zhao, Y.; Li, T.S; *Syn. Comm*., **2005**, *35*, 1859. **DOI:** 10.1081/SCC-200064898
22. Hilmy Elnagdi, N.M.; Al-Hokbany, N.S; *Molecules*. **2012**, *17*, 4300. **DOI:** 10.3390/molecules17044300
23. Wang, L.; Shao, J.; Tian, H.; Wang, Y.; Liu, B; *J. Flu. Chem*., **2006**, *127*, 97. **DOI:** 10.1016/j.jfluchem.2005.10.004
24. Khaksar, S.; Rouhollahpour, A.; Talesh, S.M; *J. Flu. Chem*., **2012**, *141*, 11. **DOI:** 10.1016/j.jfluchem.2012.05.014
25. Tahmasssebi, D.; Bryson, J.A.; Binz, S.I; *Syn. Comm*., **2011**, *41*, 2701. **DOI:** 10.1080/00397911.2010.515345
26. Gao, S.; Tsai, C.H.; Tseng, C.; Yao, C.F; *Tetrahedron*., **2008**, *64*, 9143. **DOI:** 10.1016/j.tet.2008.06.061
27. Nemouchi, S.; Boulcina, R.; Carboni, B.; Debache, A; *C.R. Chim*., **2012**, *15*, 394. **DOI:** 10.1016/j.crci.2012.01.003
28. Oskooie, H.A.; Heravi, M.M.; Karimi, N.; Zadeh, M.E; *Syn. Comm*., **2011**, *41*, 436. **DOI:** 10.1080/00397911003587499
29. Jin, T.S.; Wang, A.Q.; Wang, X.; Zhang, J.S.; Li, T.S; *Syn. Let*., **2004**, *7*, 871. **DOI:** 10.1055/s-2004-820025
30. Katkar, S.S.; Lande, M.K.; Arbad, B.R.; Gaikwad, S.T; *Chin. J. Chem*., **2011**, *29*, 199. **DOI:** 10.1002/cjoc.201190052
31. Liangce, R.; Xiaoyue, L.; Haiying, W.; Daqing, S.; Shujiang, T.; Oiya, Z; *Syn. Comm*., **2006**, *36*, 2363. **DOI:** 10.1080/00397910600640230
32. Lian, X.Z.; Huang, Y.; Li, Y.Q.; Zheng, W.J; *Monatsh. Chem*., **2008**, *139*, 129. **DOI:** 10.1007/s00706-007-0706-2
33. Babu, N.S.; Pasha, N.; Venkateswara Rao, K.T.; Prasad, P.S.S.; Lingaiah, N; *Tetrahedron Letters*., **2008**, *49*, 2730. **DOI:** 10.1016/j.tetlet.2008.02.154

Supporting Information

FTIR, ^{1}H-NMR and ^{13}C-NMR for the synthesized compounds (4a-n)

2-amino-7,7-dimethyl-5-oxo-4-phenyl-5,6,7,8-tetrahydro-4H-chromene-3-carbonitrile (4a)

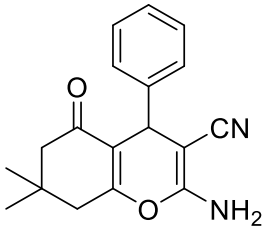

White solid, Yield: 95 %, M.P:233-235 ℃; IR (ATR, cm^{-1}): 3394 NH_2, 1036 C-N, 2201 CN, 1456 C=C, 1642 C=O, 1036 C-O, 2963 CH.
^{1}H-NMR (400 MHz, DMSO-d_6): δ (ppm) 7.26-7.30 (t, 2H, ArH). 7.12-7.17 (m, 3H, ArH), 7.00 (brs, 2H, NH2), 4.16 (s, 1H, Ar-CH), 2.49-2.51 (m, 2H, CH2), 2.01 (d, J= 14.76 Hz, 2H, CH2), 1.03 (s, 3H, CH3), 0.94 (s, 3H, -CH3).
^{13}C-NMR (400 MHz, DMSO-d_6): δ (ppm) 206.54, 195.66, 162.47, 158.45, 144.69, 128.29, 127.09, 126.53, 119.68, 112.69, 58.28, 49.93, 40.06, 35.53, 31.76, 30.64, 28.34, 26.75.

2-amino-7, 7-dimethyl-4-(4-nitrophenyl)-5-oxo-5,6,7,8-tetrahydro-4H-chromene-3-carbonitrile (4b)

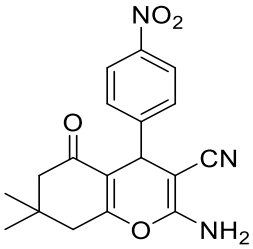

Yellow solid, Yield: 95 %, M.P: 185-187 ℃; IR (ATR, cm^{-1}): 3314 NH_2, 1043 C-N, 2191 CN, 1514 C=C, 1603 C=O, 1112 C-O, 2971 CH.
^{1}H-NMR (400 MHz, DMSO-d_6): δ(ppm) 8.15-8.17 (d, J=7.12 Hz, 2H, ArH). 7.43-7.45 (d, J= 5.36, 2H, ArH), 7.16 (brs, 2H, NH2), 4.36 (s, 1H, Ar-CH), 2.49-2.53 (t, J= 3.52 Hz, 2H, CH2), 2.23 (d, J= 16.08 Hz, 1H, CH2), 2.01 (d, J= 16.04 Hz, 1H, -CH2), 1.03 (s, 3H, CH3), 0.95 (s, 3H, -CH3).

2-amino-4-(4-fluorophenyl)-7,7-dimethyl-5-oxo-5,6,7,8-tetrahydro-4H-chromene-3-carbonitrile (4c)

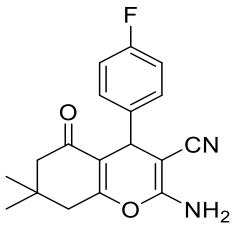

White solid, Yield: 85%, M.P:130-132 ℃; IR (ATR, cm-1): 3408 NH2, 1063 C-N, 2234 CN, 1508 C=C, 1594 C=O, 938 C-O, 3049 CH.
1H-NMR (400 MHz, CDCl3): δ (ppm) 11.85 (brs, 2H, NH2), 7.00-7.03 (m, 2H, ArH), 6.90-6.94 (m, 2H, ArH), 5.46 (s, 1H, Ar-CH), 2.31-2.41 (m, 4H, -CH2), 1.19 (s, 3H, CH3), 1.07 (s, 3H, -CH3).

2-amino-4-(4-methoxyphenyl)-7,7-dimethyl-5-oxo-5,6,7,8-tetrahydro-4H-chromene-3-carbonitrile (4d)

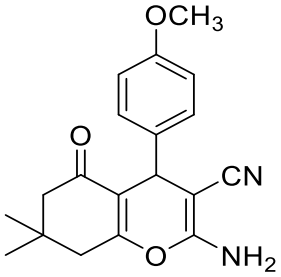

Pale yellow solid, Yield: 80 %, M.P: 212-214 ℃; IR (ATR, cm-1): 3334 NH2, 1075 C-N, 2197 CN, 1456 C=C, 1641 C=O, 1036 C-O, 2962 CH.
1H-NMR (400 MHz, CDCl3): δ (ppm) 7.11-7.13 (dd, J= 4.56 Hz, 2H, ArH). 6.78-6.80 (dd, J= 4.60 Hz, 2H, ArH), 4.48 (brs, 2H, NH2), 4.33 (s, 1H, Ar-CH), 2.41 (s, 2H, CH2), 2.18-2.19 (d, J= 5.08 Hz, 2H, CH2), 1.08 (s, 3H, CH3), 1.01 (s, 3H, -CH3).
13C-NMR (400 MHz, CDCl3): δ (ppm) 195.94, 161.21, 158.61, 157.32, 135.45, 128.62, 128.32,27. 118.76, 114.24, 113.98, 63.90,68, 52.21, 50.69, 40.67, 34.74, 32.19, 28.88.

2-amino-7,7-dimethyl-4-(2-nitrophenyl)-5-oxo-5,6,7,8-tetrahydro-4H-chromene-3-carbonitrile (4e)

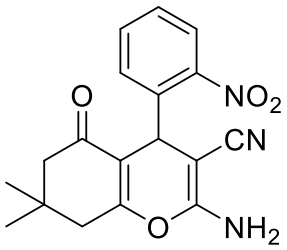

Dark yellow solid, Yield: 94 %, M.P: 234-236 ℃; IR (ATR, cm-1): 3324 NH2, 1145 C-N, 2195 CN, 1521 C=C, 1602 C=O, 1042 C-O, 2959 CH.
1H-NMR (400 MHz, DMSO-d6): δ(ppm) 7.63-7.67 (t, J= 7.56 Hz, 1H, ArH), 7.34-7.36 (t, J= 7.76 Hz, 2H, ArH), 0.87 (s, 3H, -CH3), 7.34-7.35 (d, J= 7.8 Hz, 2H, NH2), 4.93 (s, 1H, Ar-CH), 1.00 (s, 3H, CH3), 2.50 (m, 2H, CH2), 2.17-2.21 (d, J= 16.12 Hz, 1H, CH2), 1.99-2.03 (d, J= 16.12 Hz, 1H, CH2).
13C-NMR (400 MHz, DMSO-d6): δ (ppm) 196.27, 163.19, 159.65, 149.43, 139.42, 133.82, 130.74, 128.33, 124.18, 119.52, 112.78, 56.82, 50.02, 39.35, 32.30, 30.40, 28.75, 27.16.

2-amino-4-(4-chlorophenyl)-7,7-dimethyl-5-oxo-5,6,7,8-tetrahydro-4H-chromene-3-carbonitrile (4f)

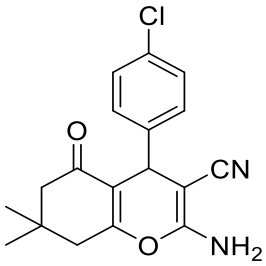

White solid, Yield: 94 %, M.P: 217-219 ℃; IR (ATR, cm^{-1}): 3330 NH_2, 1091 C-N, 2195 CN, 1607 C=C, 1643 C=O, 1038 C-O, 2969 CH.
^{1}H-NMR (400 MHz, $CDCl_3$): δ(ppm) 7.33-7.35 (d, J= 8.16 Hz, 2H, ArH), 7.16-7.18 (d, J= 8.2 Hz, 2H, ArH), 7.05 (brs, 2H, NH2), 4.19 (s, 1H, Ar-CH), 2.50 (m, 2H, CH2), 2.22-2.26 (d, J= 16.08 Hz, 1H, CH2), 2.08-2.12 (d, J= 16.04 Hz, 1H, CH2), 1.02 (s, 3H, CH3), 0.94 (s, 3H, -CH3).
^{13}C-NMR (400 MHz, $CDCl_3$): δ (ppm) 196.12, 163.07, 158.90, 144.20, 131.58, 129.57, 128.74, 120.00, 112.81, 58.27, 55.34, 50.42, 40.61, 39.36, 35.57, 32.25, 28.77, 27.33.

2-amino-7,7-dimethyl-5-oxo-4-(p-tolyl)-5,6,7,8-tetrahydro-4H-chromene-3-carbonitrile (4g)

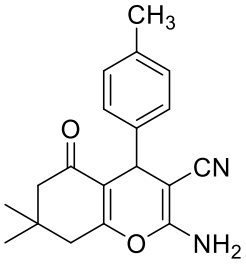

White solid, Yield: 90 %, M.P: 222-224 ℃; IR (ATR, cm^{-1}): 3333 NH_2, 1143 C-N, 2194 CN, 1512 C=C, 1603 C=O, 1037 C-O, 2961 CH.
^{1}H-NMR (400 MHz, DMSO-d_6): δ(ppm) 7.09-7.07 (d, J= 7.84, 2H, ArH), 7.00-7.02 (d, J= 7.8, 2H, ArH), 6.95 (brs, 2H, NH2), 4.12 (s, 1H, Ar-CH), 2.45-2.55 (m, J=3H, Ar-CH3), 2.22-2.26 (t, J=6.92, 4H, CH2), 1.03 (s, 3H, CH3), 0.94 (s, 3H, -CH3).
^{13}C-NMR (400 MHz, DMSO-d_6): δ (ppm) 196.10, 162.75, 158.90, 142.27, 136.08, 129.33, 127.53, 120.21, 113.34, 58.94, 50.46, 40.59, 39.75, 39.34, 35.64, 32.24, 28.88, 27.22, 21.04.

2-amino-4-(2-hydroxyphenyl)-7,7-dimethyl-5-oxo-5,6,7,8-tetrahydro-4H-chromene-3-carbonitrile (4h)

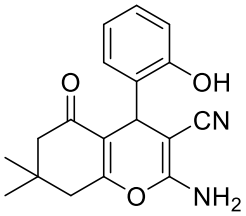

Dark brown solid, Yield: 75 %, M.P:175-177 ℃; IR (FTIR, cm^{-1}): 2958 NH_2, 1147 C-N, 2201 CN, 1579 C=C, 1642 C=O, 1025 C-O, 2900 CH.
^{1}H-NMR (400 MHz, $CDCl_3$): δ(ppm) 7.10-7.11 (m, 1H, ArH), 6.99-7.00 (m, 1.00 (s, 3H, CH3), 3H, ArH), 7.11 (brs, 2H, NH2), 4.64 (s, 1H, Ar-CH), 2.47 (s, 2H, CH2), 1.15 (s, 2H, CH2), 0.98 (s, 3H, -CH3).
^{13}C-NMR (400 MHz, $CDCl_3$): δ (ppm) 200.92, 169.17, 151.03, 127.98, 127.52, 124.58, 124.29, 118.32, 115.74, 111.03, 49.92, 41.55, 32.29, 30.95, 29.69, 29.16, 27.76, 27.18.

2-amino-4-(furan-2-yl)-7,7-dimethyl-5-oxo-5,6,7,8-tetrahydro-4H-chromene-3-carbonitrile (4i)

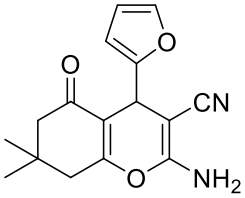

Brown solid, Yield: 94 %, M.P: 220-222 ℃; IR (FTIR, cm^{-1}): 2925 NH_2, 1174 C-N, 2224 CN, 1465 C=C, 1613 C=O, 1082 C-O, 2852 CH.
^{1}H-NMR (400 MHz, CD_3OD): δ(ppm) 7.32-7.33 (d, J= 4.0, 1H, ArH), 6.28-6.30 (m, 1H, ArH), 1.05 (s, 3H, -CH3), 6.10 (d, J= 3.16 Hz, 1H, ArH), 7.32 (brs, 2H, NH2), 4.44 (s, 1H, Ar-CH), 2.47-2.55 (q, 2H, CH2), 2.22-2.36 (q, 2H, CH2), 1.08 (s, 3H, CH3).

2-amino-6-methyl-4-phenyl-5-propionyl-4H-pyran-3-carbonitrile (4j)

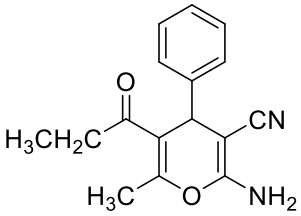

White solid, Yield: 95 %, M.P: 194-196 ℃; IR (ATR, cm^{-1}): 3395 NH_2, 1061 C-N, 2190 CN, 1411 C=C, 1693 C=O, 1121 C-O, 2970 CH.
^{1}H-NMR (400 MHz, DMSO-d_6): δ (ppm) 7.22-7.32 (t, J= 7.28, 3H, ArH). 7.18-7.22 (t, J= 8.08 Hz, 1H, ArH), 7.13-7.15 (d, J= 7.04 Hz, 2H, ArH), 6.89 (brs, 2H, NH2), 4.28 (s, 1H, Ar-CH), 3.94-3.97 (m, 2H, -CH2),), 2.12 (s, 3H, CH3), 1.00-1.03 (t, J= 7.08, 3H, -CH3).
^{13}C-NMR (400 MHz, DMSO-d_6): δ (ppm) 206.48, 165.40, 158.43, 156.55, 144.83, 128.39, 127.14, 126.77, 119.68, 107.20, 60.10, 57.21, 38.82, 30.62, 18.07 13.66.

2-amino-6-methyl-4-(4-nitrophenyl)-5-propionyl-4H-pyran-3-carbonitrile (4k)

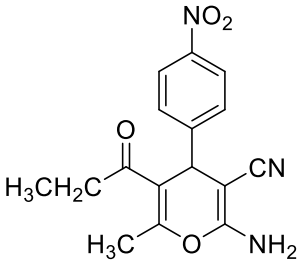

Yellow solid, Yield: 94 %, M.P: 177-179 ℃; IR (ATR, cm^{-1}): 3406 NH_2, 1120 C-N, 2201 CN, 1519 C=C, 1682 C=O, 1055 C-O, 2985 CH.

^{1}H-NMR (400 MHz, DMSO-d_6): δ (ppm) 8.17-8.20 (d, J= 8.67 Hz, 2H, ArH). 7.42-7.44 (d, J= 8.63 Hz, 2H, ArH), 7.06 (brs, 2H, NH2), 4.46 (s, 1H, Ar-CH), 3.92-3.97 (m, 2H, -CH2), 2.34 (s, 3H, CH3), 0.99-1.02 (t, J= 7.12, 3H, -CH3).
^{13}C-NMR (400 MHz, DMSO-d_6): δ (ppm) 165.05, 158.52, 157.90, 152.51, 146.35, 128.50, 123.77, 119.29, 105.95, 60.33, 56.10, 39.99, 38.73, 18.27, 13.64.

2-amino-4-(4-fluorophenyl)-6-methyl-5-propionyl-4H-pyran-3-carbonitrile (4l)

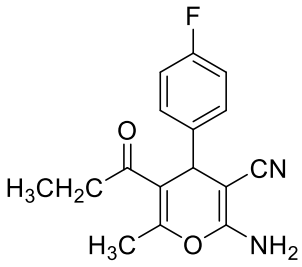

White solid, Yield: 83 %, M.P:159-161 ℃; IR (ATR, cm^{-1}): 3407 NH_2, 1094 C-N, 2194 CN, 1508 C=C, 1605 C=O, 1057 C-O, 2985 CH.
^{1}H-NMR (400 MHz, $CDCl_3$): δ(ppm) 7.32-7.35 (m, 2H, ArH), 7.13-7.18 (t, J= 8.52 Hz, 2H, ArH), 7.24 (brs, 2H, NH2), 3.91-3.96 (m, 1H, Ar-CH), 2.59 (s, 2H, -CH3), 2.14 (s, 2H, CH2), 0.85-089 (t, J= 7.12, 3H, -CH3).

2-amino-6-methyl-4-(2-nitrophenyl)-5-propionyl-4H-pyran-3-carbonitrile (4m)

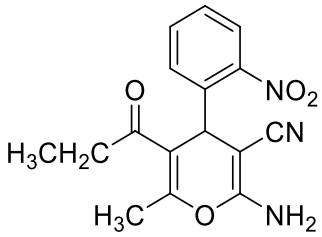

Dark yellow solid, Yield: 94 %, M.P: 176-178 ℃; IR (ATR, cm^{-1}): 3455 NH_2, 1127 C-N, 2209 CN, 1525 C=C, 1602 C=O, 1064 C-O, 2987 CH.
^{1}H-NMR (400 MHz, $CDCl_3$): δ(ppm) 7.67-7.69 (t, J= 6.72, 1H, ArH), 7.47-7.48 (m, 1H, ArH), 7.43-7.47 (m, 2H, ArH), 7.42 (brs, 2H, NH2), 5.01 (s, 1H, Ar-CH), 3.85-3.90 (m, J=6.92, 2H, CH2), 2.84 (s, 3H, OCH3), 0.89-0.92 (t, J= 7.08, 3H, -CH3).
^{13}C-NMR (400 MHz, $CDCl_3$): δ (ppm) 164.79, 158.93, 158.25, 148.47, 139.55, 133.73, 130.41, 128.06, 123.70, 118.91, 106.30, 60.25, 55.8532.83, 18.27, 13.43.

2-amino-6-methyl-5-propionyl-4-(p-tolyl)-4H-pyran-3-carbonitrile (4n)

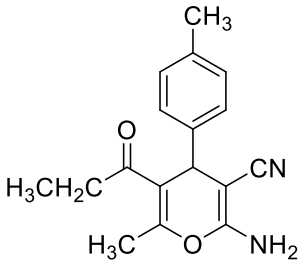

White solid, Yield: 75 %, M.P: 121-123 ℃; IR (FTIR, cm^{-1}): 3049 NH_2, 1133 C-N, 2229 CN, 1575 C=C, 1615 C=O, 1046 C-O, 2979 CH.
^{1}H-NMR (400 MHz, $CDCl_3$): δ(ppm) 7.95-7.97 (t, J= 8.92, 2H, ArH) 7.15-7.18 (t, J= 7.08, 2H, ArH), 4.48 (brs, 2H, NH2), 4.38 (s, 1H, Ar-CH), 4.01- 4.03 (m, 2H, CH2), 2.33 (s, 3H, Ar-CH3), 2.27 (s, 3H, CH3), 1.01-1.07 (t, J= 7.16, 3H, -CH3).
^{13}C-NMR (400 MHz, $CDCl_3$): δ (ppm) 207.46, 165.99, 157.61, 156.58, 140.87, 136.71, 129.69, 129.24, 127.38, 119.14, 108.13, 62.21, 60.64, 38.29, 30.90, 21.04, 18.38.

2-amino-7,7-dimethyl-5-oxo-4-phenyl-5,6,7,8-tetrahydro-4H-chromene-3-carbonitrile (4a)

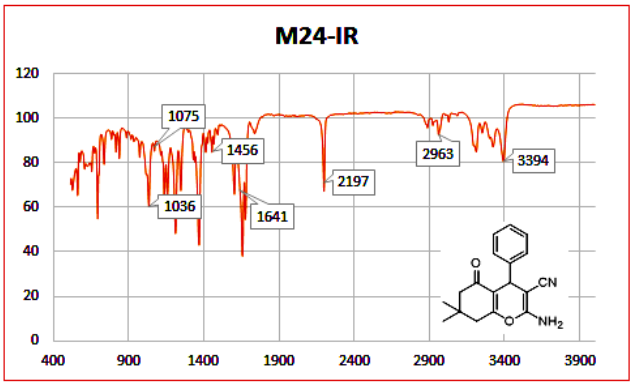

Fig. S 1. IR spectrum for 4a.

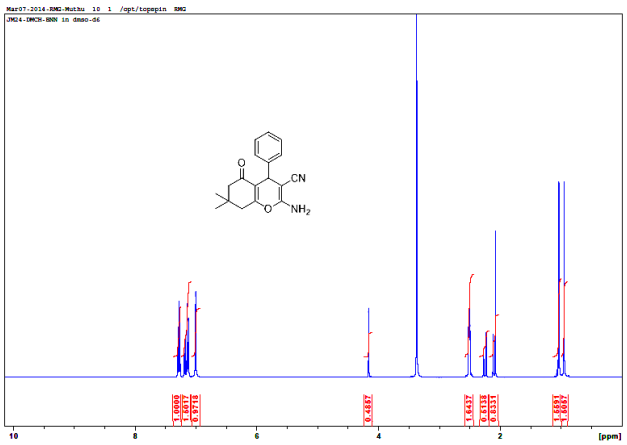

Fig. S 2. ^{1}H-NMR Spectrum for **4a.**

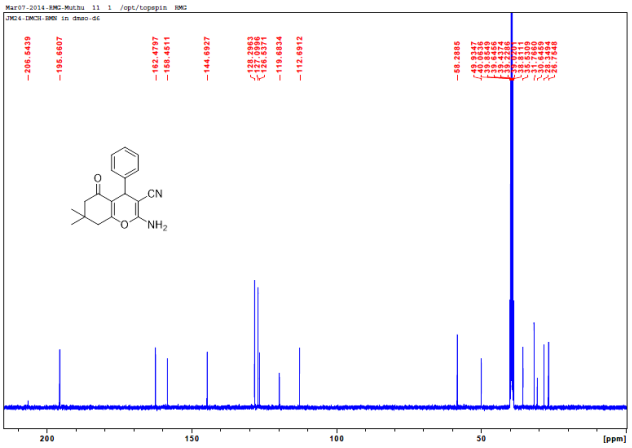

Fig. S 3. 13C-NMR Spectrum for 4a.

2-amino-7,7-dimethyl-4-(4-nitrophenyl)-5-oxo-5,6,7,8-tetrahydro-4H-chromene-3-carbonitrile (4b)

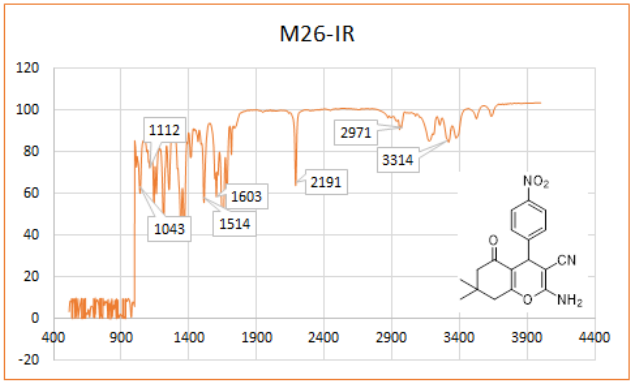

Fig. S 4. IR spectrum for **4b.**

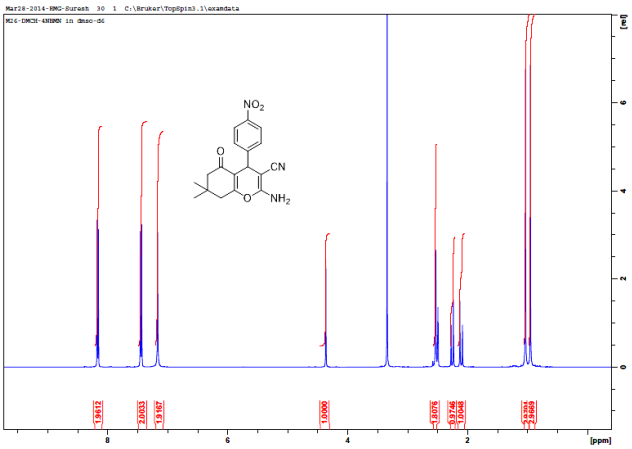

Fig. S 5. ^{1}H-NMR Spectrum for **4b.**

2-amino-4-(4-fluorophenyl)-7,7-dimethyl-5-oxo-5,6,7,8-tetrahydro-4H-chromene-3-carbonitrile (4c)

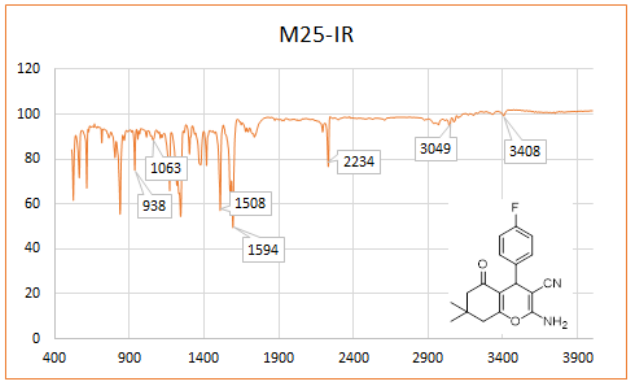

Fig. S 6. IR spectrum for **4c.**

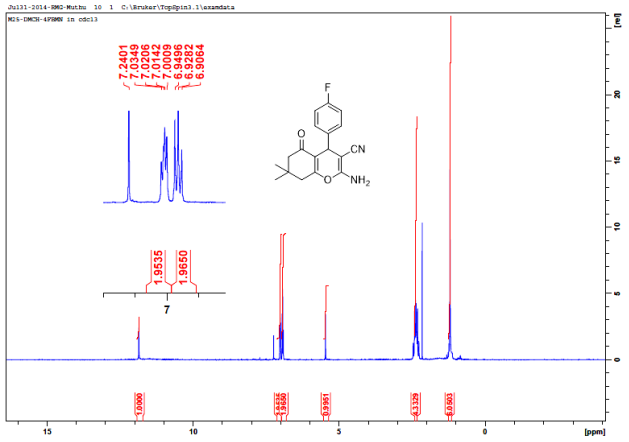

Fig. S 7. ^{1}H-NMR Spectrum for **4c.**

2-amino-4-(4-methoxyphenyl)-7,7-dimethyl-5-oxo-5,6,7,8-tetrahydro-4H-chromene-3-carbonitrile (4d)

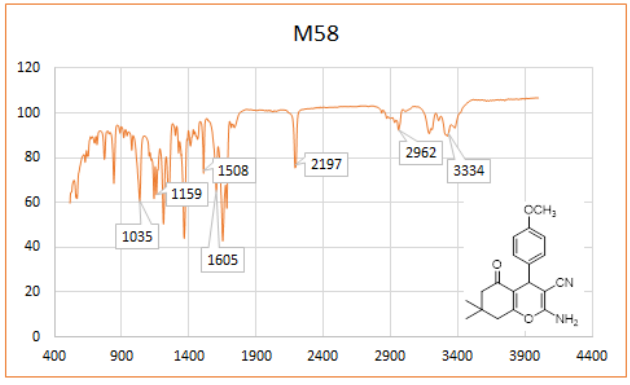

Fig. S 8. IR spectrum for **4d.**

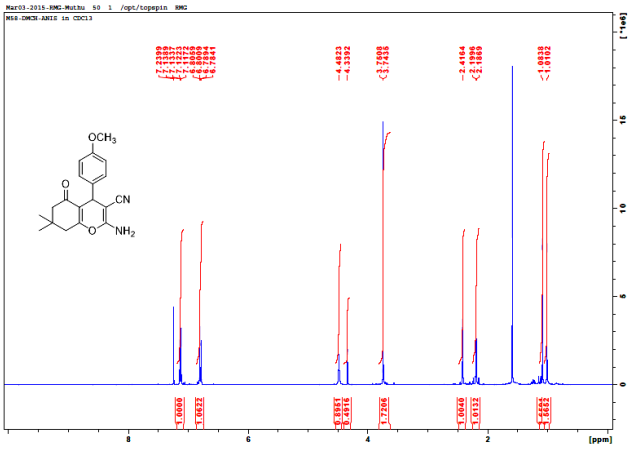

Fig. S 9. ^{1}H-NMR Spectrum for **4d**

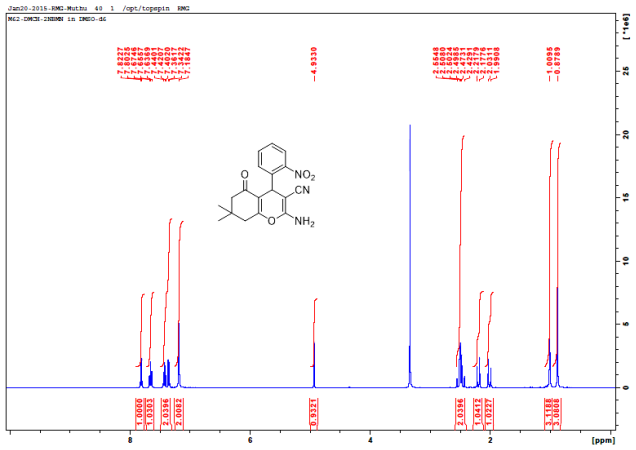

Fig. S 12. ^{1}H-NMR Spectrum for **4e.**

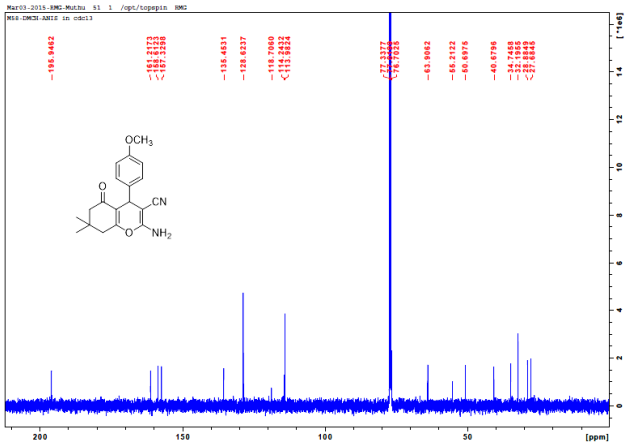

Fig. S 10. ^{13}C-NMR Spectrum for **4d**

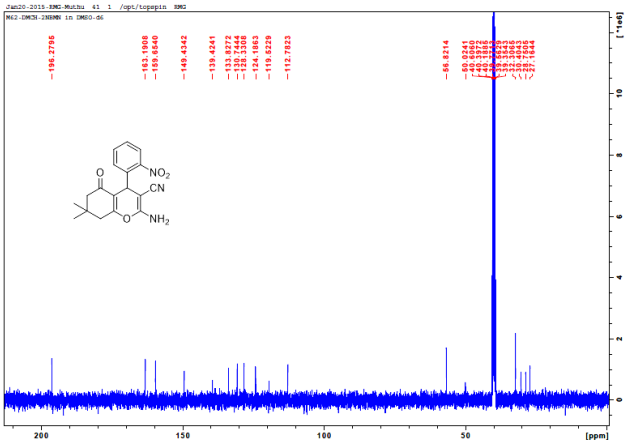

Fig. S 13. ^{13}C-NMR Spectrum for **4e**

2-amino-7,7-dimethyl-4-(2-nitrophenyl)-5-oxo-5,6,7,8-tetrahydro-4H-chromene-3-carbonitrile (4e)

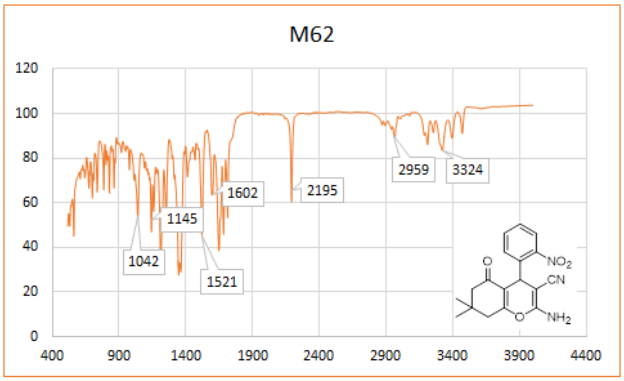

Fig. S 11. IR spectrum for **4e.**

2-amino-4-(4-chlorophenyl)-7,7-dimethyl-5-oxo-5,6,7,8-tetrahydro-4H-chromene-3-carbonitrile (4f)

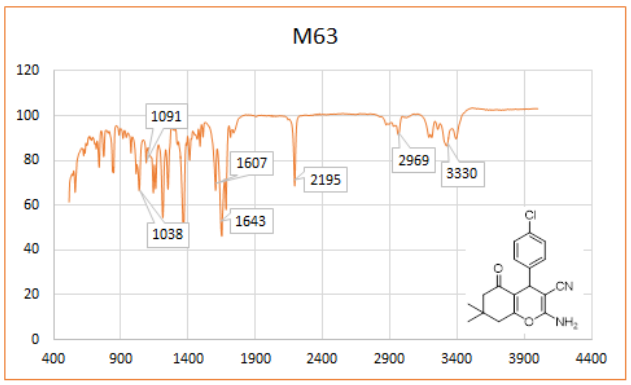

Fig. S 14. IR spectrum for **4f**

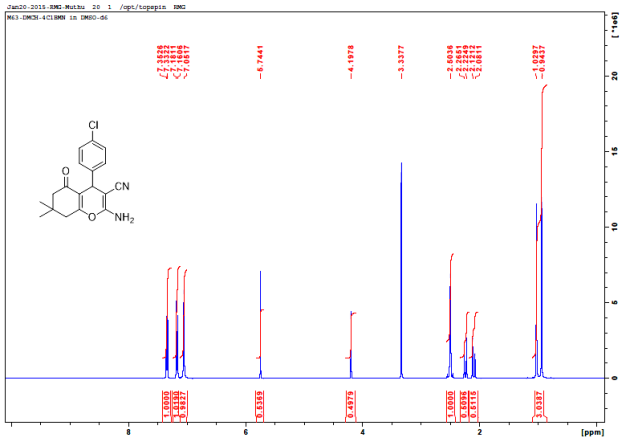

Fig. S 15. ^{1}H-NMR Spectrum for **4f**

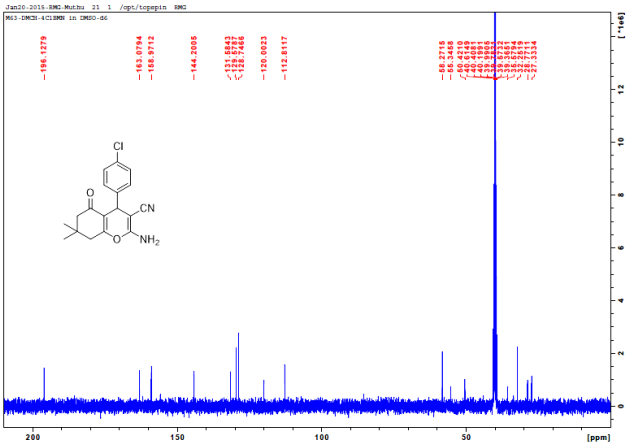

Fig. S 16. ^{13}C-NMR Spectrum for **4f**

2-amino-7,7-dimethyl-5-oxo-4-(p-tolyl)-5,6,7,8-tetrahydro-4H-chromene-3-carbonitrile (4g)

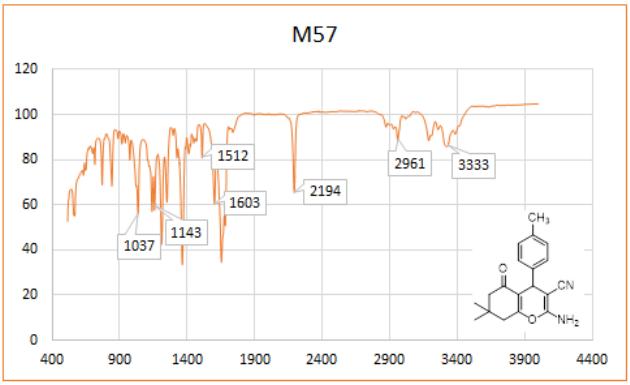

Fig. S 17. IR spectrum for **4g**

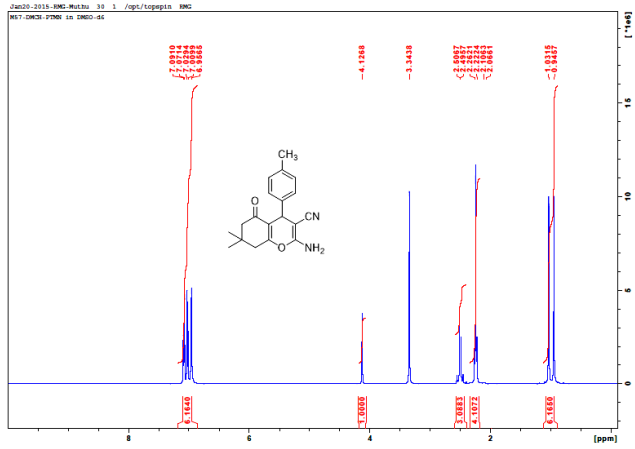

Fig. S 18. ^{1}H-NMR Spectrum for **4g**

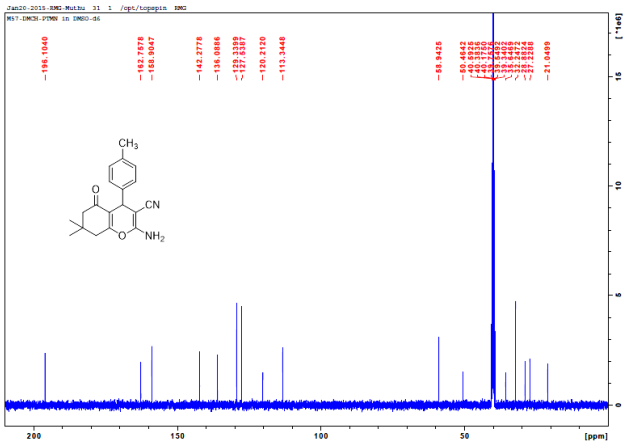

Fig. S 19. ^{13}C-NMR Spectrum for **4g**

2-amino-4-(2-hydroxyphenyl)-7,7-dimethyl-5-oxo-5,6,7,8-tetrahydro-4H-chromene-3-carbonitrile (4h)

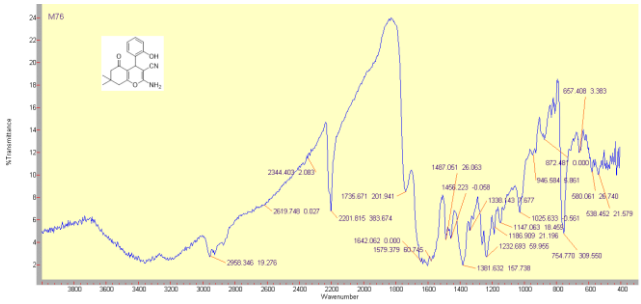

Fig.S 20. IR spectrum for **4h**

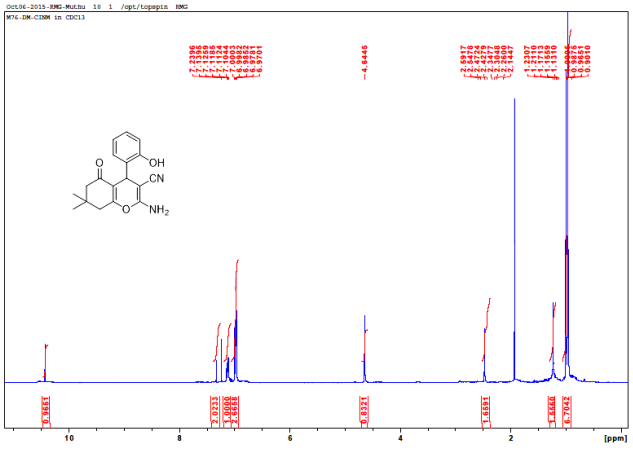

Fig. S 21. ^{1}H-NMR Spectrum for **4h**

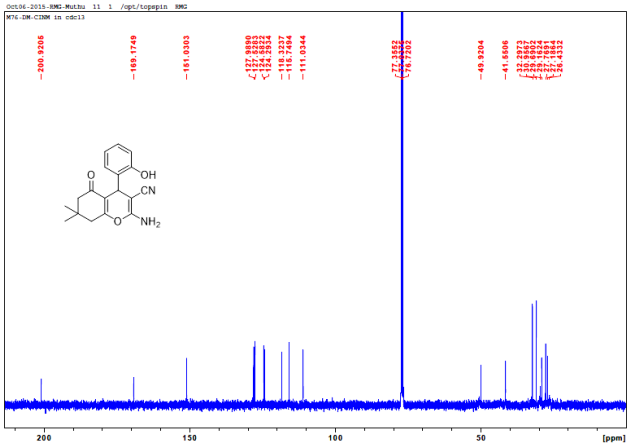

Fig. S 22. ^{13}C-NMR Spectrum for **4h**

2-amino-4-(furan-2-yl)-7,7-dimethyl-5-oxo-5,6,7,8-tetrahydro-4H-chromene-3-carbonitrile (4i)

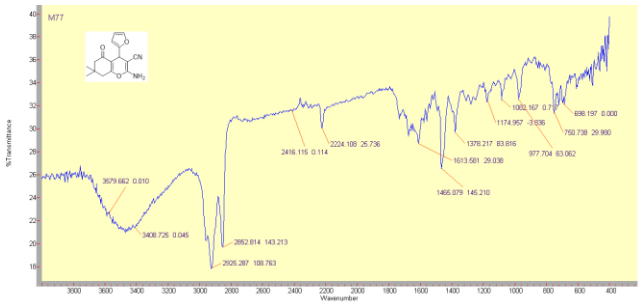

Fig. S 23. IR spectrum for **4i**

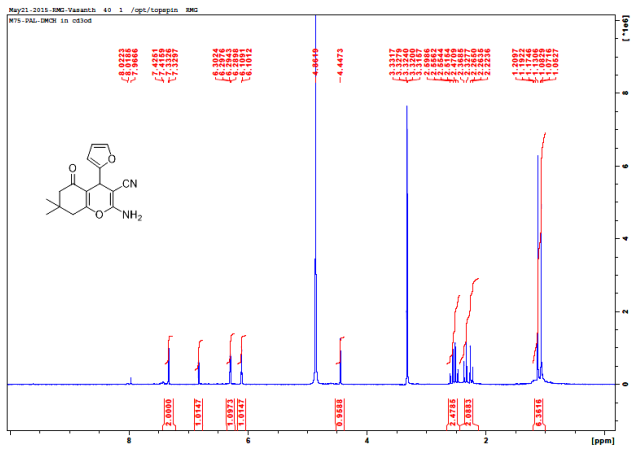

Fig. S 24. ^{1}H-NMR Spectrum for **4i**

2-amino-6-methyl-4-phenyl-5-propionyl-4H-pyran-3-carbonitrile (4j)

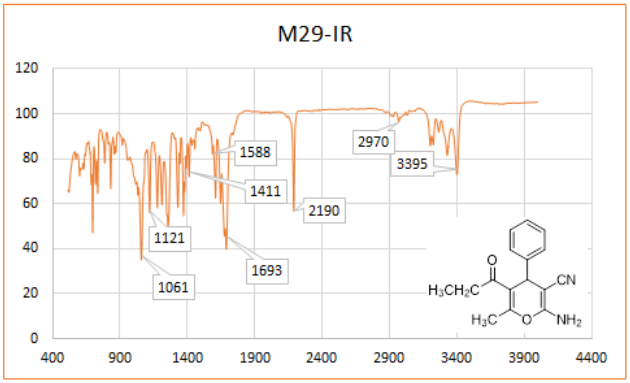

Fig. S 25. IR spectrum for **4j**

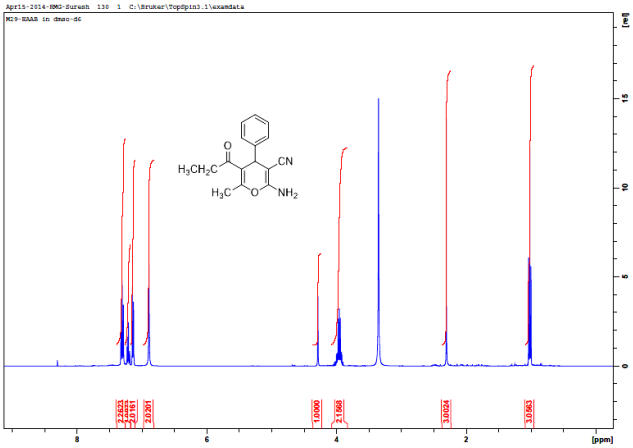

Fig. S 26. ^{1}H-NMR Spectrum for **4j**

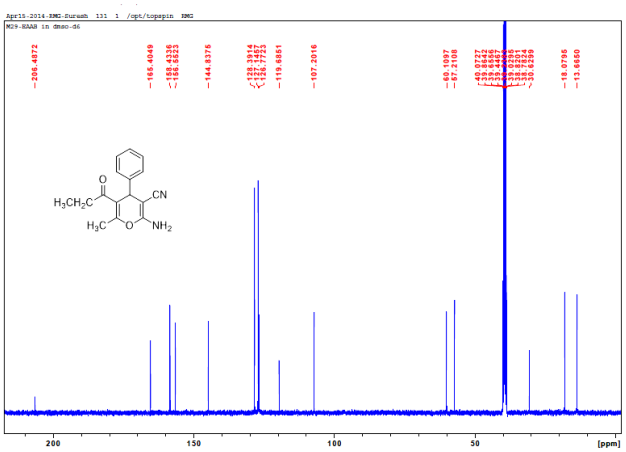

Fig. S 27. ^{13}C-NMR Spectrum for **4j**

2-amino-6-methyl-4-(4-nitrophenyl)-5-propionyl-4H-pyran-3-carbonitrile (4k)

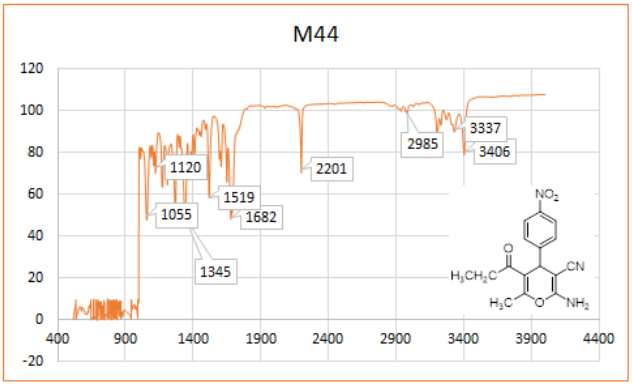

Fig. S 28. IR spectrum for **4k**

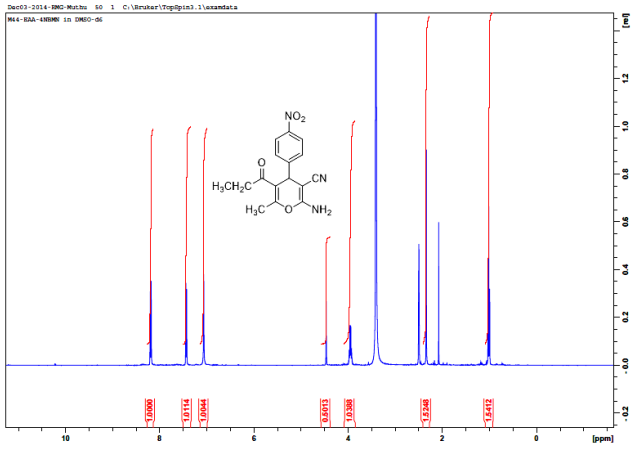

Fig. S 29. ^{1}H-NMR Spectrum for **4k**

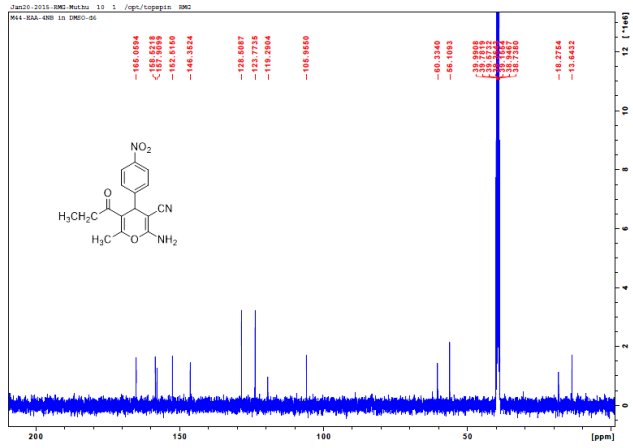

Fig. S 30. ^{13}C-NMR Spectrum for **4k**

2-amino-4-(4-fluorophenyl)-6-methyl-5-propionyl-4H-pyran-3-carbonitrile (4l)

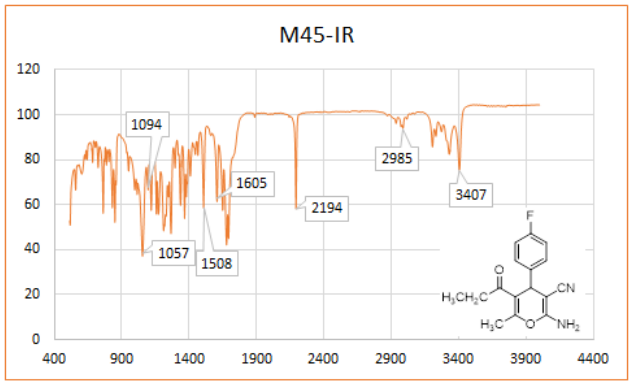

Fig. S 31. IR spectrum for **4l**

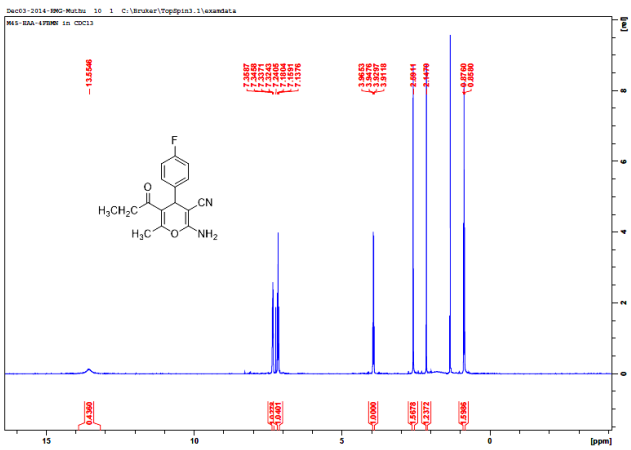

Fig. S 32. ^{1}H-NMR Spectrum for **4l**

2-amino-6-methyl-4-(2-nitrophenyl)-5-propionyl-4H-pyran-3-carbonitrile (4m)

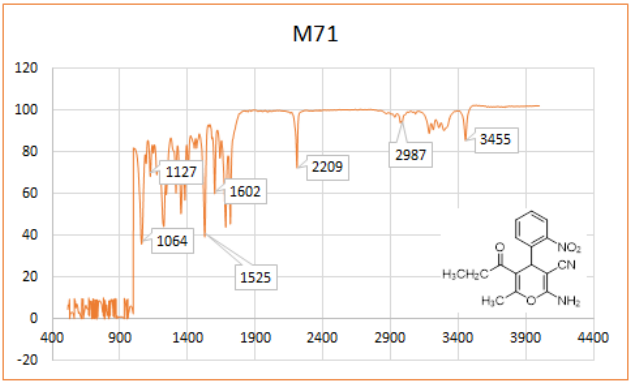

Fig. S 33. IR Spectrum for **4m**

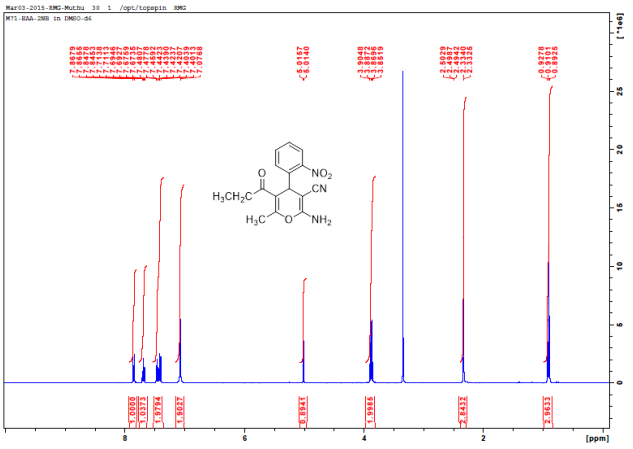

Fig. S 34. ^{1}H-NMR Spectrum for **4m**

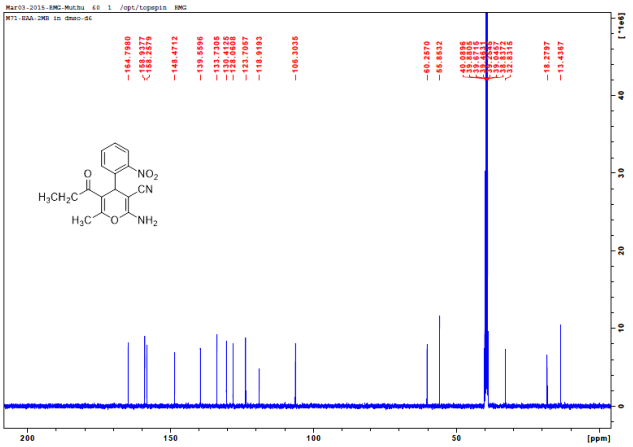

Fig. S 35. ^{13}C-NMR Spectrum for **4m**

2-amino-6-methyl-5-propionyl-4-(p-tolyl)-4H-pyran-3-carbonitrile (4n)

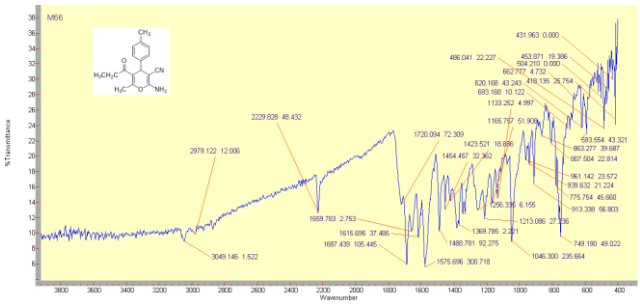

Fig. S 36. IR spectrum for **4n**

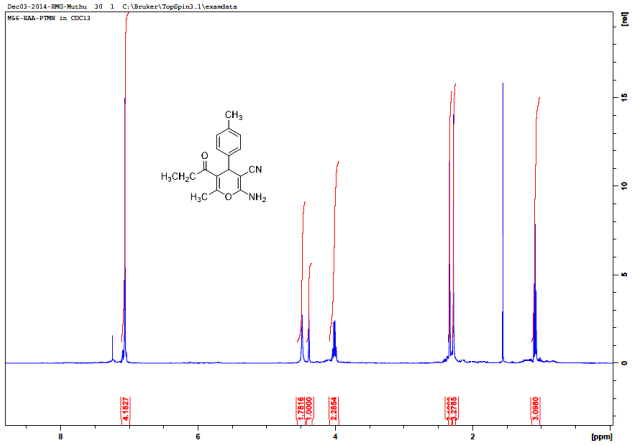

Fig. S 37. ^{1}H-NMR Spectrum for **4n**

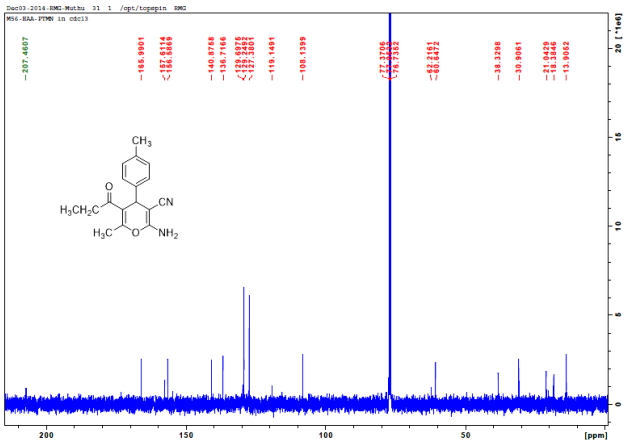

Fig. S 38. ^{13}C-NMR Spectrum for **4n**